

Understanding the magnetic ground state of rare-earth intermetallic compound Ce_4Sb_3 : Magnetization and neutron diffraction studies

R. Nirmala ^{a,*}, A.V. Morozkin ^b, O. Isnard ^{c,d}, A.K. Nigam ^e

^a Department of Physics, Indian Institute of Technology Madras, Chennai 600 036, Tamil Nadu, India

^b Department of Chemistry, Moscow Lomonosov State University, Moscow, Russia

^c Institut Laue-Langevin, 6 Rue J. Horowitz, 38042 Grenoble, France

^d Laboratoire de Cristallographie du CNRS, Université J. Fourier, BP166X, 38042 Grenoble, France

^e Tata Institute of Fundamental Research, Mumbai 400 005, India

ARTICLE INFO

Article history:

Received 17 July 2008

Available online 28 August 2008

Keywords:

Rare-earth intermetallic compound and alloy

Magnetic property

Neutron diffraction

Magnetocaloric effect

ABSTRACT

Magnetization and neutron diffraction studies have been performed on Ce_4Sb_3 compound (cubic Th_3P_4 -type, space group $\text{I}\bar{4}3\text{d}$, no. 220). Magnetization of Ce_4Sb_3 reveals a ferromagnetic transition at ~ 5 K, the temperature below which the zero-field-cooled and field-cooled magnetization bifurcate in low applied fields. However, a saturation magnetization (M_S) value of only $\sim 0.93\mu_B/\text{Ce}^{3+}$ is observed at 1.8 K, suggesting possible presence of crystal field effects and a paramagnetic/antiferromagnetic Ce^{3+} moment. Magnetocaloric effect in this compound has been computed using the magnetization vs. field data obtained in the vicinity of the magnetic transition, and a maximum magnetic entropy change, $-\Delta S_M$, of $\sim 8.9\text{ J/kg/K}$ is obtained at 5 K for a field change of 5 T. Inverse magnetocaloric effect occurs at ~ 2 K in 5 T indicating the presence of antiferromagnetic component. This has been further confirmed by the neutron diffraction study that evidences commensurate antiferromagnetic ordering at 2 K in zero magnetic field. A magnetic moment of $\sim 1.24\mu_B/\text{Ce}^{3+}$ is obtained at 2 K and the magnetic moments are directed along Z-axis.

© 2008 Elsevier B.V. All rights reserved.

1. Introduction

Magnetocaloric properties of various rare-earth intermetallic compounds and transition metal oxides are being more actively explored of late owing to their possible applicability in energy-efficient magnetic refrigeration technology [1–3]. To meet low-temperature and near-room-temperature cooling demands, suitable candidate materials for a broad working temperature range of 4–300 K are being sought. Ce-based intermetallic compounds and alloys, in general, are known to display interesting physical properties such as heavy fermion behaviour, valence fluctuation and Kondo behaviour. The Ce_4Sb_3 compound has cubic Th_3P_4 -type structure (space group $\text{I}\bar{4}3\text{d}$, no. 220) at room temperature [4,5]. This compound is known to exhibit ground-state ferromagnetic properties in competition with Kondo interaction [6,7]. The isostructural Ce_4Bi_3 compound displays a first-order transition to a ferromagnetic state at ~ 3.5 K.

In the present work, magnetization measurements were performed on polycrystalline Ce_4Sb_3 in magnetic fields up to 5 T. In addition, neutron diffraction study in zero field has been

carried out down to 1.8 K. The magnetization results indicate that a ferromagnetic order sets in at ~ 5 K (T_C) in Ce_4Sb_3 compound. Furthermore, a persisting antiferromagnetic component seems to exist at 1.8 K within the ferromagnetically ordered state. Neutron diffraction data at 2 K indeed confirm an antiferromagnetic spin arrangement at 2 K.

2. Experimental

The polycrystalline Ce_4Sb_3 compound was prepared in an electric arc furnace under argon atmosphere using a non-consumable tungsten electrode and a water-cooled copper tray. Antimony (purity 99.999 wt%) and cerium (purity 99.9 wt%) were used as the starting components. Zirconium was used as a getter during the melting process. The quality of the sample was determined using X-ray powder diffraction and analysis by scanning electron microscopy (SEM) equipped with EDX microprobe analysis. (A “Camebax” microanalyser was employed to perform microprobe X-ray spectral analyses of the specimen.)

X-ray powder diffraction pattern was obtained on a diffractometer DRON-3 (CuK α -radiation, $2\theta = 20\text{--}90^\circ$, step 0.05°). The obtained diffractogram was identified and intensity calculations were made in the isotropic approximation using the

* Corresponding author.

E-mail address: nirmala100@gmail.com (R. Nirmala).

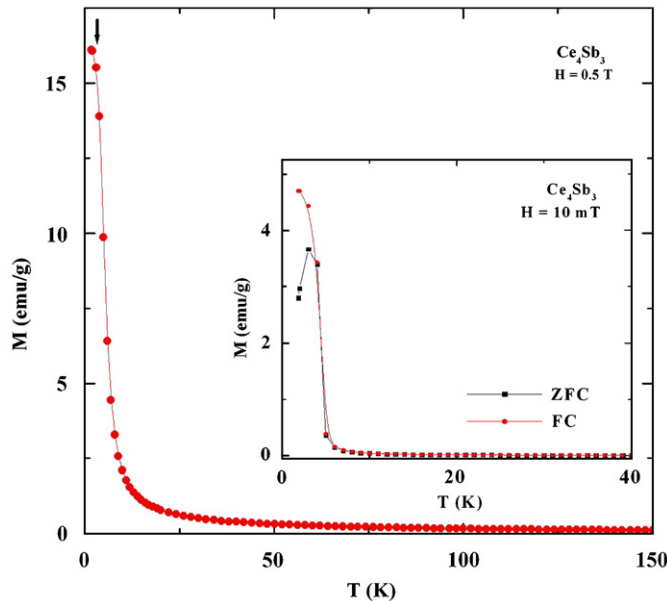


Fig. 1. Temperature dependence of magnetization, $M(T)$, of Ce_4Sb_3 compound in 0.5 T field (inset: zero-field-cooled and field-cooled magnetization of Ce_4Sb_3 as a function of temperature in 10 mT field).

Rietan-program [8]. The neutron diffraction investigation was carried out from 26 K to 2 K in zero applied magnetic field at the Institute Laue-Langevin, Grenoble, France, using the high-resolution powder diffractometer D1B [9], operating at a wavelength $\lambda = 0.252$ nm ($2\theta = 2.8\text{--}84^\circ$). The diffraction patterns were indexed and the calculations performed by using the FULLPROF 98-program [10]. DC magnetization studies were carried out using commercial SQUID magnetometer (MPMS, Quantum Design, USA) in the temperature range of 1.8–300 K, in magnetic fields up to 5 T.

3. Results and discussion

Room temperature X-ray diffraction pattern confirms the formation of single-phase cubic Th_3P_4 -type Ce_4Sb_3 (space group $\text{I}\bar{4}3\text{d}$, no. 220) compound. The temperature variation of magnetization of Ce_4Sb_3 is measured in 0.5 T applied field (Fig. 1). These data reveal that this compound orders ferromagnetically at ~ 5 K. In an applied field of 10 mT, the zero-field-cooled (ZFC) and field-cooled (FC) magnetization data branch off below 5 K (inset in Fig. 1). In general, the difference between ZFC and FC magnetization implies possible competing interactions in the compound, spin glass nature or domain wall pinning in narrow domain wall systems. The magnetic ordering temperature value of 5 K is in agreement with that of the earlier study [4]. The paramagnetic susceptibility follows Curie–Weiss law with a paramagnetic Curie temperature (θ_P) of ~ -6 K and an effective paramagnetic moment (μ_{eff}) of $\sim 3\mu_B/\text{Ce}^{3+}$. The negative θ_P value points to the presence of competing antiferromagnetic and ferromagnetic interactions. The effective paramagnetic moment value is slightly larger than that of theoretical estimate for free ion Ce^{3+} ($g[J(J+1)]^{1/2}$) is $\sim 2.54\mu_B/\text{Ce}^{3+}$.

Though a ferromagnetic-like ordering is observed at 5 K, the magnetization vs. field (M - H) isotherm obtained at 1.8 K yields a saturation magnetization (M_S) value of only $\sim 0.93\mu_B/\text{Ce}^{3+}$ in 5 T field (Fig. 2). This is much less than that expected from the theoretical Ce^{3+} free ion value of $2.14\mu_B$ (g). Magnetization

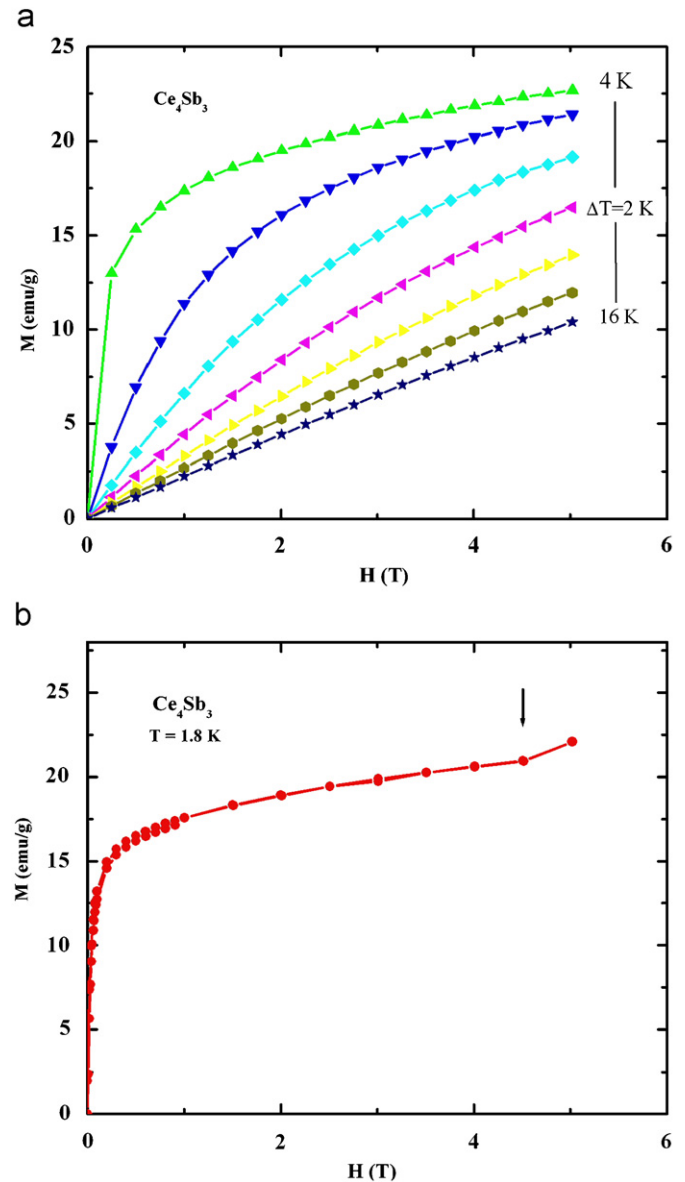


Fig. 2. Magnetization vs. field isotherms at various temperatures in the temperature range of 20–1.8 K, in fields up to 5 T.

changes its slope around 4.5 T and increases steeply up to 5 T. Hence, a possible field-induced, high-field state which is more ferromagnetically ordered is not ruled out.

In order to examine the ground-state magnetic structure of Ce_4Sb_3 compound, a powder neutron diffraction study was undertaken. Typical powder neutron diffraction patterns in the paramagnetic state and magnetically ordered state were obtained at temperatures 26 and 2 K (Fig. 3), respectively. The neutron diffraction pattern at 2 K shows the development of commensurate reflections (110) and (330) that correspond to long-range antiferromagnetic structure. The details of the magnetic structure at 2 K are given in Fig. 4 and Table 1. The positions of Ce atoms in the unit cell are given in Table 2. Fig. 4 shows that the magnetic sublattice consists of two identical Ce sublattices (Ce1, 2, 3, 4, 9, 10, 11, 12 and Ce5, 6, 7, 8, 13, 14, 15, 16). The shortest Ce1, 2, 3, 4–Ce9, 10, 11, 12 (Ce5, 6, 7, 8–Ce13, 14, 15, 16) distance is 0.3678 nm, which is close to the sum of Ce atomic radii ($R_{\text{Ce}} = 0.1825$ nm [11]), whereas Ce1, 2, 3, 4, 9, 10, 11,

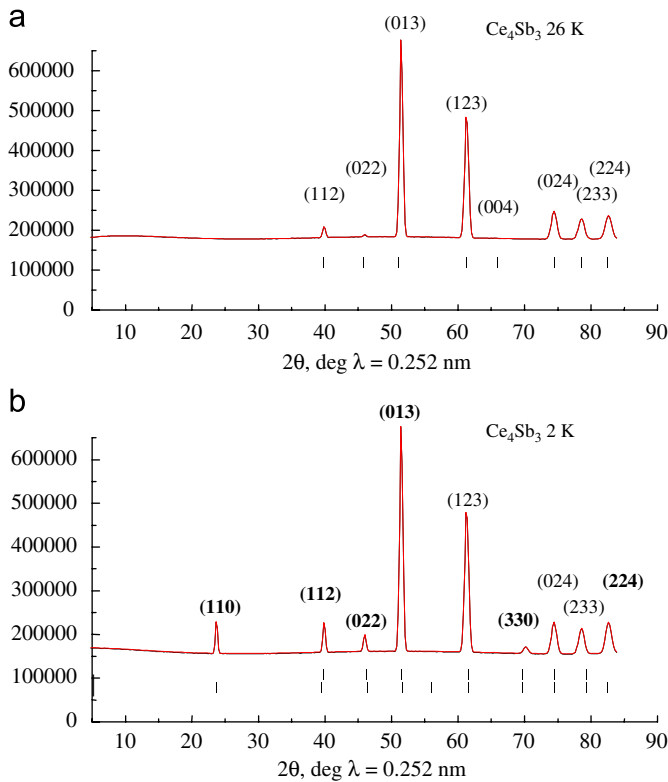


Fig. 3. Powder neutron diffraction pattern of Ce_4Sb_3 at 26 K (paramagnetic state) (a) and at 2 K (magnetically ordered state) (b).

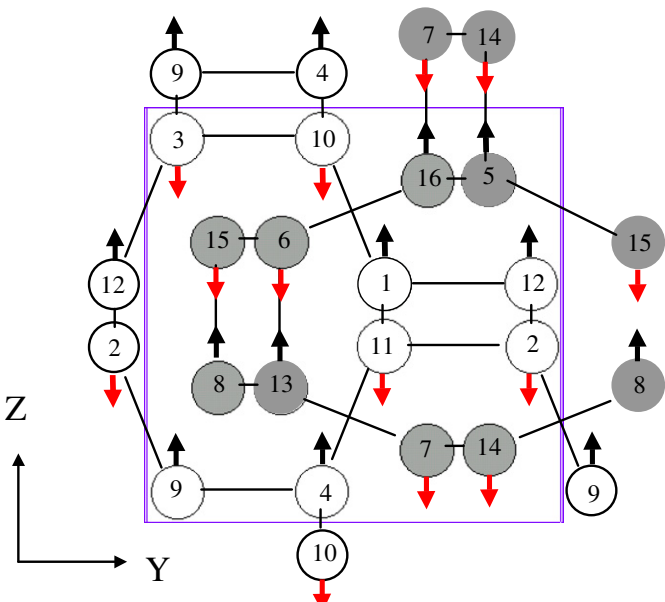


Fig. 4. Magnetic structure of Ce_4Sb_3 at 2 K in zero field. (Projection of Th_3P_4 -type unit cell on YZ plane. Sb atoms are not shown for the sake of clarity.) The shortest Ce-Ce distances are marked and Ce1, 2, 3, 4, 9, 10, 11, 12 and Ce5, 6, 7, 8, 13, 14, 15, 16 moments are indicated in the figure.

12–Ce5, 6, 7, 8, 13, 14, 15, 16 distance is 0.4122 nm at room temperature.

The magnetic moment at Ce site is found to be $1.24(1)\mu_B/\text{Ce}^{3+}$, somewhat larger than that observed by magnetization data, yet

Table 2
Atomic positions of Ce atoms in the Th_3P_4 -type Ce_4Sb_3 unit cell

Atom	X/a	Y/b	Z/c
Ce1	X_{Ce}	X_{Ce}	X_{Ce}
Ce2	$X_{\text{Ce}}-1/2$	$3/2-X_{\text{Ce}}$	$1-X_{\text{Ce}}$
Ce3	$1-X_{\text{Ce}}$	$X_{\text{Ce}}-1/2$	$3/2-X_{\text{Ce}}$
Ce4	$3/2-X_{\text{Ce}}$	$1-X_{\text{Ce}}$	$X_{\text{Ce}}-1/2$
Ce5	$X_{\text{Ce}}+1/4$	$X_{\text{Ce}}+1/4$	$X_{\text{Ce}}+1/4$
Ce6	$3/4-X_{\text{Ce}}$	$X_{\text{Ce}}-1/4$	$5/4-X_{\text{Ce}}$
Ce7	$X_{\text{Ce}}-1/4$	$5/4-X_{\text{Ce}}$	$3/4-X_{\text{Ce}}$
Ce8	$5/4-X_{\text{Ce}}$	$3/4-X_{\text{Ce}}$	$X_{\text{Ce}}-1/4$
Ce9	$X_{\text{Ce}}-1/2$	$X_{\text{Ce}}-1/2$	$X_{\text{Ce}}-1/2$
Ce10	X_{Ce}	$1-X_{\text{Ce}}$	$3/2-X_{\text{Ce}}$
Ce11	$3/2-X_{\text{Ce}}$	X_{Ce}	$1-X_{\text{Ce}}$
Ce12	$1-X_{\text{Ce}}$	$3/2-X_{\text{Ce}}$	X_{Ce}
Ce13	$X_{\text{Ce}}-1/4$	$X_{\text{Ce}}-1/4$	$X_{\text{Ce}}-1/4$
Ce14	$5/4-X_{\text{Ce}}$	$1/4+X_{\text{Ce}}$	$3/4-X_{\text{Ce}}$
Ce15	$1/4+X_{\text{Ce}}$	$3/4-X_{\text{Ce}}$	$5/4-X_{\text{Ce}}$
Ce16	$3/4-X_{\text{Ce}}$	$5/4-X_{\text{Ce}}$	$1/4+X_{\text{Ce}}$

not closer to the Ce tripositive free ion magnetic moment. The Ce moments are directed along Z -axis of a cubic unit cell.

The magnetocaloric effect in this compound near 5 K has been evaluated using the M - H data obtained in the vicinity of the magnetic transition (Fig. 5). The Arrot plots (M^2 vs. H/M) suggest that the magnetic transition at 5 K is of second order (figure not shown). The magnetic entropy change associated with the transition, ΔS_M , has been calculated from isothermal magnetization measurements performed at small, discrete field intervals at different temperatures near T_c , using the following formula:

$$|\Delta S_M| = \sum_i \frac{M_i - M_{i+1}}{T_{i+1} - T_i} \Delta H \quad (1)$$

where M_i and M_{i+1} are the values of magnetization at temperatures T_i and T_{i+1} , respectively. A maximum magnetic entropy change is found to be $\sim 8.9 \text{ J/kg/K}$ at 5 K, for a field change of 5 T. The sign of magnetocaloric effect changes at 1.8 K in 5 T field, confirming the existence of antiferromagnetic component within the ferromagnetically ordered state. It is worth to recall that the earlier report on heat capacity data of Ce_4Sb_3 compound has observed a T^3 dependence of heat capacity below T_c and suggested strengthening of antiferromagnetic spin wave stiffness in applied magnetic field [7]. High-field magnetization measurements are in progress. The structure and magnetic properties of Ce_4Sb_3 compound are summarized in Table 3.

Thus, magnetism of Ce_4Sb_3 system indeed shows interesting features such as presence of competing magnetic interactions and their significance in various regions of the temperature–field phase diagram as depicted by their magnetic properties.

4. Conclusions

The magnetic and magnetocaloric properties of Ce_4Sb_3 compound have been studied down to 1.8 K. Isothermal magnetic entropy change of magnitude $\sim 9 \text{ J/kg/K}$ is obtained close to 5 K, the ferromagnetic transition temperature. Existence of the antiferromagnetic component in Ce_4Sb_3 at 1.8 K is evidenced by both magnetic and neutron diffraction measurements.

Table 1

Crystallographic and magnetic parameters of Ce_4Sb_3 compound: cell parameter a , atomic position parameters X_{Ce} , magnetic moment of the Ce atom M_{Ce} at different temperatures T

Fig.	T_N (K)	State	T (K)	a (nm)	X_{Ce}	R_F (%)	M_{Ce} (μ_B)	Atom	θ ($^\circ$)	R_F^m (%)
		Para ^a	300	0.95190(6)	0.5699(3)	6.1				
			26	0.9560(2)	0.5705(5)	2.2				
2	<14	AF	2	0.9560(2)	0.5710(6)	2.2	1.24(1)	Ce1,4,5,8,9,12,13,16 Ce2,3,6,7,10,11,14,15	0 180	8.7

θ is the angle of Ce magnetic moment with Z-axis of the unit cell. The temperature T_N refers to a magnetic transition from neutron diffraction experiment. Reliability factors R_F (crystal structure) and R_F^m (magnetic structure) are given in percent (%).

^a X-ray data.

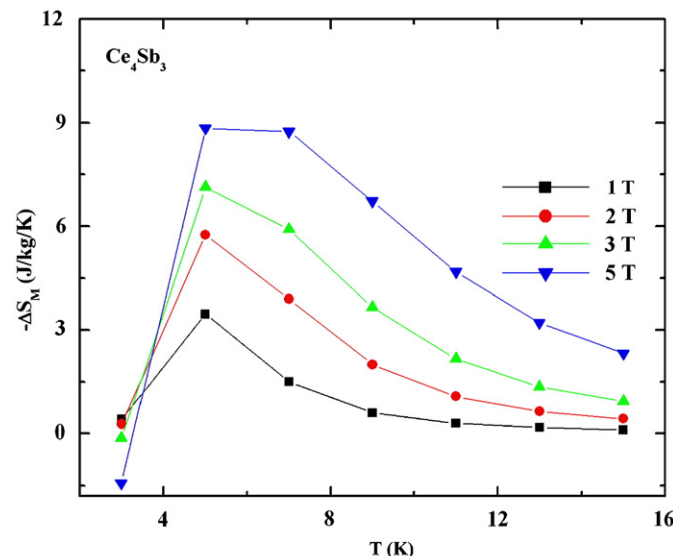


Fig. 5. Magnetic entropy change, $-\Delta S_M$, in Ce_4Sb_3 compound as a function of temperature for various field changes.

Table 3

Crystallographic and magnetic properties of Th_3P_4 -type Ce_4Sb_3 compound

Structure type	Th_3P_4
Space group	I43d, c128, no. 220
Cell parameter a , nm at 300 K	0.95190(6)
Atomic positions (at 300 K)	16 (c) Ce [0.5699(3), $X_{\text{Ce}}, X_{\text{Ce}}]$
Paramagnetic temperature Θ_p (K)	-6
Effective paramagnetic moment (μ_B/Ce^{3+})	3
Curie temperature T_C (K)	5
Critical field H_C (T)	4.5
Saturation magnetization, M_S (μ_B)	0.93
Magnetic structure at 2 K in zero field (neutron diffraction)	Commensurate antiferromagnetic
Magnetic moment at 2 K in zero field, M_{Ce}^2 (μ_B) (from neutron diffraction)	1.24(1)
Magnetocaloric effect at 5 K, for 5 T field change $ \Delta S_M $ (J/kg K)	8.85

Acknowledgements

This work was supported by the Russian Fund for Basic Research through Project No. 06-08-00233-a. The present work has also been supported by the Institut Laue-Langevin (Grenoble, France) by Experiment No. 5-31-1789. R.N. thanks IIT Madras for support under research Grant No. Phy/07-08/222/NFSC/RNIR. The authors thank P. Henry (Institut Laue-Langevin, Grenoble, France) and P. Manfrinetti (Dipartimento di Chimica, Università di Genova, Italy) for help in the neutron diffraction experiment.

References

- [1] V. Provenzano, A.J. Shapiro, R.D. Shull, Nature (London) 429 (2004) 854.
- [2] O. Tegus, E. Brück, K.H.J. Buschow, F.R. de Boer, Nature 415 (2002) 150.
- [3] K.A. Gschneidner Jr., V.K. Pecharsky, A.O. Tsokol, Rep. Prog. Phys. 68 (2005) 1479.
- [4] P.I. Kripyakevich, Sov. Phys. Cryst. 7 (1963) 556.
- [5] F. Holtzberg, T.R. Macguire, S. Methfessel, J.C. Suits, J. Appl. Phys. 35 (1964) 1033.
- [6] A. Ochiai, Y. Nakabayashi, Y.S. Kwon, K. Takeuchi, K. Takegahara, T. Suzuki, T. Kasuya, J. Magn. Magn. Mater. 52 (1985) 304.
- [7] T. Suzuki, O. Nakamura, N. Tomonaga, S. Ozeki, Y.S. Kwon, A. Ochiai, T. Takeda, T. Kasuya, Physica B 163 (1990) 131.
- [8] F. Izumi, R.A. Young (Eds.), The Rietveld Method, Oxford University Press, Oxford, 1993 (Chapter 13).
- [9] www.ill.fr, Yellow Book.
- [10] J. Rodriguez-Carvajal, Physica B 192 (1993) 55.
- [11] J. Emsley, in: The Elements, second ed., Clarendon Press, Oxford, 1991.